Human Molecular Genetics, 2013, Vol. 22, No. 10 **2105–2118**
doi:10.1093/hmg/ddt060
Advance Access published on February 12, 2013

A novel interaction between FRMD7 and CASK: evidence for a causal role in idiopathic infantile nystagmus

Rachel J. Watkins[1], Rajashree Patil[1], Benjamin T. Goult[1], Mervyn G. Thomas[2], Irene Gottlob[2] and Sue Shackleton[1,*]

[1]Department of Biochemistry, University of Leicester, Leicester LE1 9HN, UK and [2]Ophthalmology group, School of Medicine, University of Leicester, PO Box 65, Leicester LE2 7LX, UK

Received December 18, 2012; Revised and Accepted February 5, 2013

Idiopathic infantile nystagmus (IIN) is a genetically heterogeneous disorder of eye movement that can be caused by mutations in the *FRMD7* gene that encodes a FERM domain protein. FRMD7 is expressed in the brain and knock-down studies suggest it plays a role in neurite extension through modulation of the actin cytoskeleton, yet little is known about its precise molecular function and the effects of IIN mutations. Here, we studied four IIN-associated missense mutants and found them to have diverse effects on FRMD7 expression and cytoplasmic localization. The C271Y mutant accumulates in the nucleus, possibly due to disruption of a nuclear export sequence located downstream of the FERM-adjacent domain. While overexpression of wild-type FRMD7 promotes neurite outgrowth, mutants reduce this effect to differing degrees and the nuclear localizing C271Y mutant acts in a dominant-negative manner to inhibit neurite formation. To gain insight into FRMD7 molecular function, we used an IP-MS approach and identified the multi-domain plasma membrane scaffolding protein, CASK, as a FRMD7 interactor. Importantly, CASK promotes FRMD7 co-localization at the plasma membrane, where it enhances CASK-induced neurite length, whereas IIN-associated FRMD7 mutations impair all of these features. Mutations in CASK cause X-linked mental retardation. Patients with C-terminal CASK mutations also present with nystagmus and, strikingly, we show that these mutations specifically disrupt interaction with FRMD7. Together, our data strongly support a model whereby CASK recruits FRMD7 to the plasma membrane to promote neurite outgrowth during development of the oculomotor neural network and that defects in this interaction result in nystagmus.

INTRODUCTION

Idiopathic infantile nystagmus (IIN) is an inherited oculomotor disorder involving involuntary oscillations of the eyes, often leading to reduced visual function and with a reported prevalence of 2.4 in 10 000 (1–3). There is currently no curative treatment for nystagmus and the molecular basis of the disease is poorly understood. It has been postulated that IIN results from a primary developmental defect in the region of the brain responsible for oculomotor control (4), although there is currently limited direct evidence to support this.

IIN has varied inheritance patterns, suggesting the involvement of multiple genes, although the majority of cases are X-linked and two of the five nystagmus loci are located on the X chromosome at Xp11.4–p11.3 (5) and Xq26–q27 (6), respectively. Nystagmus can occur as a secondary phenotype associated with other genetic disorders such as ocular albinism, which is linked to mutations in the G-protein-coupled receptor GPR143 (7), and is also occasionally observed in patients with X-linked mental retardation, caused by mutations in the MAGUK family scaffolding-protein CASK (8).

*To whom correspondence should be addressed at: Department of Biochemistry, Henry Wellcome Building, University of Leicester, Leicester LE1 9HN, UK. Tel: +44 116 229 7058; Fax: +44 116 229 7018; Email: ss115@le.ac.uk

To date, only one gene associated with IIN has been cloned and this is the *FRMD7* gene, located at Xq26 (9). Mutations in *FRMD7* are the major cause of familial IIN and idiopathic infantile periodic alternating nystagmus (9,10). Patients with *FRMD7* mutations also have variably reduced visual acuity and abnormal optokinetic response (3,10,11). The basis of the phenotypic variability among affected subjects is currently unclear.

FRMD7 encodes a member of the FERM domain family of plasma membrane–cytoskeleton coupling proteins, named after the founding members of the family: protein 4.1, ezrin, radixin and moesin (12). As in most other FERM-domain family members, the conserved FERM domain of FRMD7 is located at the N-terminus and is divided into three lobes (denoted either as lobes A–C or F1–F3) that form a cloverleaf structure. This domain is usually responsible for membrane association through interaction with integral membrane proteins and lipids. In contrast to the N-terminus, the C-terminal domain of FRMD7 bears no significant homology to other proteins. FRMD7 also has a central FERM-adjacent (FA) domain that is found in a subset of FERM domain proteins, and which has been found to regulate protein function through modifications such as phosphorylation (13). Many FERM domain proteins have been shown to bind directly to actin or to other components of the actin cytoskeleton, usually via their divergent non-FERM-domain regions and are thought to be involved in localized regulation of actin dynamics (reviewed in 14).

The closest homologs of FRMD7, FARP1 and FARP2, play roles in neuronal development through regulation of neurite outgrowth and guidance (15–18), leading to speculation that FRMD7 may play a role in development of the oculomotor neural circuitry. In support of this, FRMD7 is highly expressed in regions of the developing brain that are involved in oculomotor control, as well as in the retina (9,19). Furthermore, FRMD7 has been shown to co-localize with actin in the primary neurites of differentiating Neuro2A cells and knockdown of FRMD7 in these cells leads to a reduction in average neurite length (20).

IIN-associated mutations in FRMD7 are highly clustered within the N-terminal region of the protein, indicating that the FERM and FA domains are likely to be critical to FRMD7 function (21). Almost half of the mutations are predicted to cause premature protein termination, leading to the suggestion that IIN results from loss of protein expression and/or function in affected males. However, the effects of missense mutations, which account for around 53% of IIN mutations, have not been investigated. Furthermore, the precise molecular pathways involving FRMD7 during neuronal differentiation are currently unknown.

In the present study, we sought to investigate the effects of four IIN-associated missense mutations on FRMD7 expression and its ability to promote neurite outgrowth. We found that all mutants examined disrupt expression, localization and/or neurite outgrowth to varying degrees. We also sought to identify FRMD7 interacting proteins as a means of gaining insight into the molecular pathways involving FRMD7 in neuronal cells and identified the MAGUK family member, CASK, as a binding partner of FRMD7. Importantly, we show that nystagmus-associated mutations in FRMD7 disrupt the interaction with CASK, preventing their co-localization at the plasma membrane and impairing CASK-induced neurite formation. Our findings highlight the importance of the FRMD7–CASK interaction in promoting membrane extension during neurite outgrowth.

RESULTS

IIN-associated mutations disturb FRMD7 protein expression and localization

To address the role of FRMD7 in nystagmus, we generated a range of human IIN-associated myc-tagged and GFP-tagged FRMD7 mutants. We chose to focus on four point mutations located in the FERM and FA domains (Fig. 1A), rather than frame-shift and truncation mutations, since they were more likely to retain at least partial expression and function and therefore give insight into disease mechanisms. Transient expression of the GFP-tagged mutants in Neuro2A cells revealed that three of the mutants (G24E, R229C and C271Y) had a lower level of expression compared with wild-type (WT) FRMD7, suggesting that these mutations may reduce protein stability (Fig. 1B). In contrast, the S340L mutant had a similar expression level to WT FRMD7.

We generated a structural homology model of the FRMD7 FERM domain (residues 1–280) using PHYRE (22) and the highly homologous FERM domain of protein 4.1R (Fig. 1C). The side-chain of C271 is located within the center of the F3 sub-domain and mutation to tyrosine results in the insertion of a bulky side-chain into this restricted region of the protein, which is likely to destabilize the protein and potentially alter the binding surface of F3 (9). G24E is also likely to destabilize the protein by addition of a larger charged residue into the core of the F1 sub-domain. In contrast, R229 is a surface-exposed polar residue and consequently its mutation to cysteine (R229C) is unlikely to result in protein instability. Interestingly, R229 is located in a highly basic region of the F3 sub-domain and the removal of one of the basic charges may disrupt its binding site for interacting partners or with the phospholipid membrane. S340 lies outside of the FERM domain, immediately downstream of the FA domain and so the effect of the S340L mutation could not be modeled.

Immunofluorescence microscopy using myc-tagged FRMD7 mutants revealed that, like WT FRMD7, the G24E, R229C and S340L mutants were predominantly cytoplasmic, although a low level of nuclear expression was also apparent (Fig. 1D). Surprisingly, however, we found that the C271Y mutant was concentrated in the nucleus in most cells.

Thus, the four mutants analyzed appear to have markedly different effects on FRMD7 protein expression and localization.

FRMD7 contains a nuclear export sequence that regulates uptake into the nucleus

To further investigate the potential mechanism of FRMD7 C271Y localization to the nucleus, we generated FRMD7 deletion mutants to identify which domain of the protein might be involved in determining cytoplasmic versus nuclear localization. Myc-FRMD7 mutants encompassing the FERM domain alone (FERM), the FERM plus FA domains (FERM + FA) and C-terminal domain (CTD) were transiently expressed in Neuro2A cells and their subcellular localization studied by immunofluorescence microscopy 24 and 48 h post-

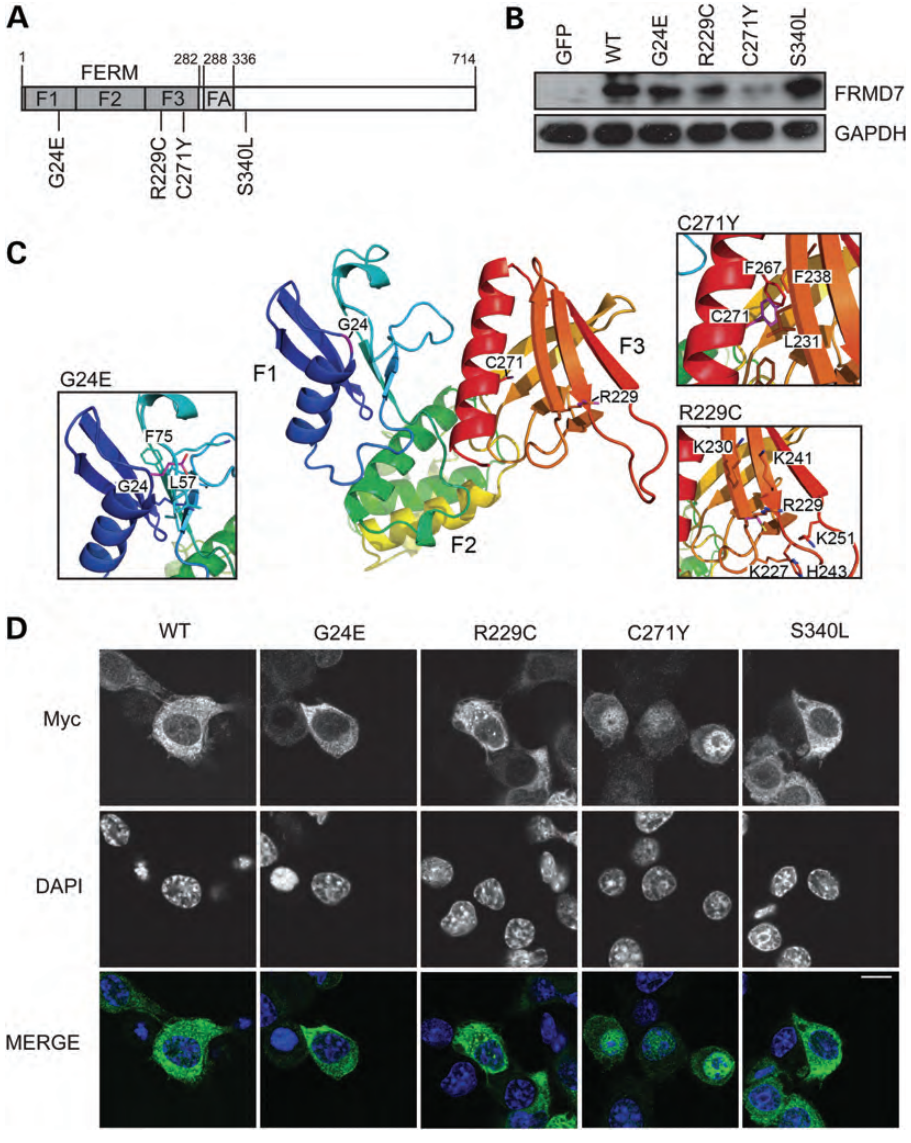

Figure 1. IIN-associated mutations disrupt FRMD7 protein expression and localization. (**A**) Schematic representation of the domain organization of FRMD7, containing an N-terminal FERM domain, comprising F1, F2 and F3 lobes, and FERM-adjacent (FA) domain. Locations of IIN-associated mutations used in the study are indicated. Sequences are based on the 714-residue FRMD7 isoform (ENST00000298542). (**B**) Neuro2A cells were transiently transfected with GFP-tagged WT or mutant FRMD7. Cell lysates were immunoblotted with anti-FRMD7 and anti-GAPDH antibodies. (**C**) Structural model of the FRMD7 FERM domain highlighting the location of the mutations G24E, R229C and C271Y. Insets depict magnified regions of the three mutations; in each case, the sidechain of the mutated residue is shown in magenta. (**D**) Neuro2A cells were seeded onto coverslips, transiently transfected with myc-tagged WT or mutant FRMD7 and fixed in methanol. Immunofluorescence microscopy was then performed using anti-myc antibodies (green in merged image) and DAPI to stain chromatin (blue in merged image). Cells with higher expression were chosen for imaging to allow clear visualization of protein localization and are therefore not representative of expression level. Scale bar, 10 μm.

transfection (Fig. 2). We found that FRMD7-CTD was localized almost entirely within the cytoplasm at both time-points, in a similar manner to WT FRMD7. Conversely, FRMD7-FERM+FA was distributed between both the cytoplasm and nucleus, with a slight enrichment in the nucleus, and at 48 h cells became noticeably rounded up, with distorted nuclei. Although not obviously concentrated in the nucleus, FRMD7-FERM had an even more pronounced effect on cell morphology, with rounding up of cells and highly distorted nuclei evident at 24 h post-transfection. Although suggestive of apoptosis, these cells were negative for cleaved caspase-3, indicating that the morphological changes observed were not simply an indicator of cell death (data not shown). These results indicate that the conserved N-terminal regions of FRMD7 are responsible for nuclear localization and that expression of the N-terminus alone has a dominant-negative effect on cell morphology.

Since WT FRMD7 is predominantly cytoplasmic, but does show a low level of nuclear staining under normal culture conditions (Fig. 1C), we reasoned that the protein may be capable of import into the nucleus but that accumulation in the nucleus may be prevented by dominance of an export mechanism. To test this possibility, we treated cells expressing myc-FRMD7 with leptomycin B, which inhibits the exportin CRM1. Under these conditions, FRMD7 accumulated in the nucleus (Fig. 3A), confirming that the protein can undergo nuclear import, but that

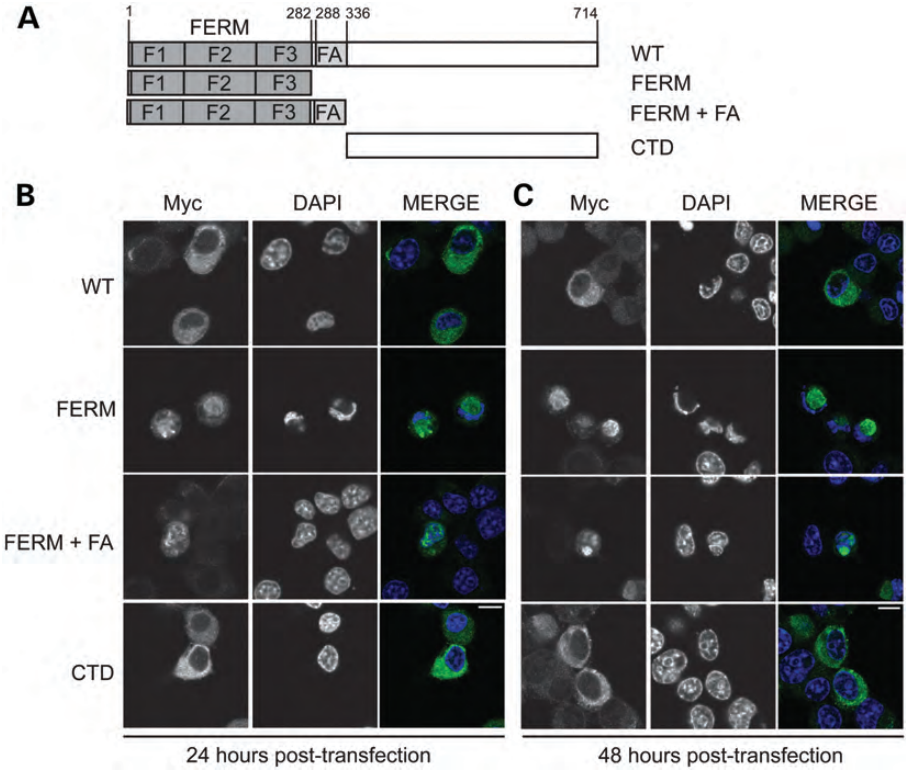

Figure 2. The N-terminus of FRMD7 determines nuclear localization. (**A**) Schematic representation of the FRMD7 deletion constructs used in this study. (**B** and **C**) Neuro2A cells were seeded onto coverslips, transiently transfected with myc-tagged WT or mutant FRMD7 and fixed in methanol 24 (B) or (C) 48 h later. Immunofluorescence microscopy was then performed using anti-myc antibodies (green in merged image) and DAPI to stain chromatin (blue in merged image). Scale bar, 10 μm.

nuclear export predominates under normal culture conditions. FRMD7 remained predominantly cytoplasmic in differentiating Neuro2A cells treated with retinoic acid (RA) for 24 or 48 h, indicating that FRMD7 does not translocate to the nucleus during neuronal differentiation (data not shown).

Our data suggested that sequences within the N-terminal region may control nuclear localization of FRMD7. Examination of the amino-acid sequence revealed a potential nuclear localization signal (NLS) at residues 234–237, within lobe F3 of the FERM domain, and CRM1-dependent leucine-rich nuclear export sequence (NES) at residues 344–356, immediately downstream of the FA domain (Fig. 3B). To determine whether these motifs are bona fide targeting sequences, we mutated critical residues within each motif. To inactivate the NES, we mutated leucines 354 and 356 to serine. The NES mutant showed significant accumulation in the nucleus compared with WT FRMD7 (Fig. 3C), confirming that residues 354 and 356 do play an important role in the export of FRMD7 from the nucleus by forming a part of a CRM1-dependent NES. In contrast, mutation of the putative NLS sequence had no effect on nuclear accumulation of FRMD7 in the presence of leptomycin B, suggesting that nuclear import is achieved by an alternative mechanism (data not shown).

Overexpression of FRMD7 mutants inhibits the formation and extension of neurites

Current evidence suggests that FRMD7 is likely to play a role in neurite outgrowth during brain development. We therefore investigated the effects of IIN-associated mutations on this process by observing the extent of neurite growth in RA-treated Neuro2A cells transiently expressing myc-tagged FRMD7 proteins (Fig. 4). First, we found that exogenous expression of WT FRMD7 led to a 2-fold increase in the number of neurites and average neurite length per cell when compared with mock-transfected control cells. Furthermore, there was a 7-fold increase in the extent of neurite branching in the presence of FRMD7. These data confirm that FRMD7 has a positive effect on neurite outgrowth and branching.

The IIN-associated mutations G24E, R229C and C271Y abrogated the ability of FRMD7 to enhance average neurite length, suggesting that these mutants are non-functional with respect to neurite extension. The G24E and R229C mutants also caused a significant reduction in the number of neurites and the level of branching, although they were generally still slightly enhanced compared with control cells, again suggesting that these mutants retained little functional activity. Strikingly, expression of the C271Y mutant caused a significant reduction in the number of neurites, when compared with mock-transfected cells, indicating that this mutant has a dominant-negative effect on neurite formation. In contrast, the S340L mutant had no effect on either the number of neurites or the extent of branching. Average neurite length was reduced in cells expressing the S340L mutant, but remained enhanced compared with mock-transfected cells, indicating a partial loss of function. These results demonstrate that all of the IIN-associated mutations had a common effect on reducing overall neurite length, but that the extent of inhibition varied for each mutant.

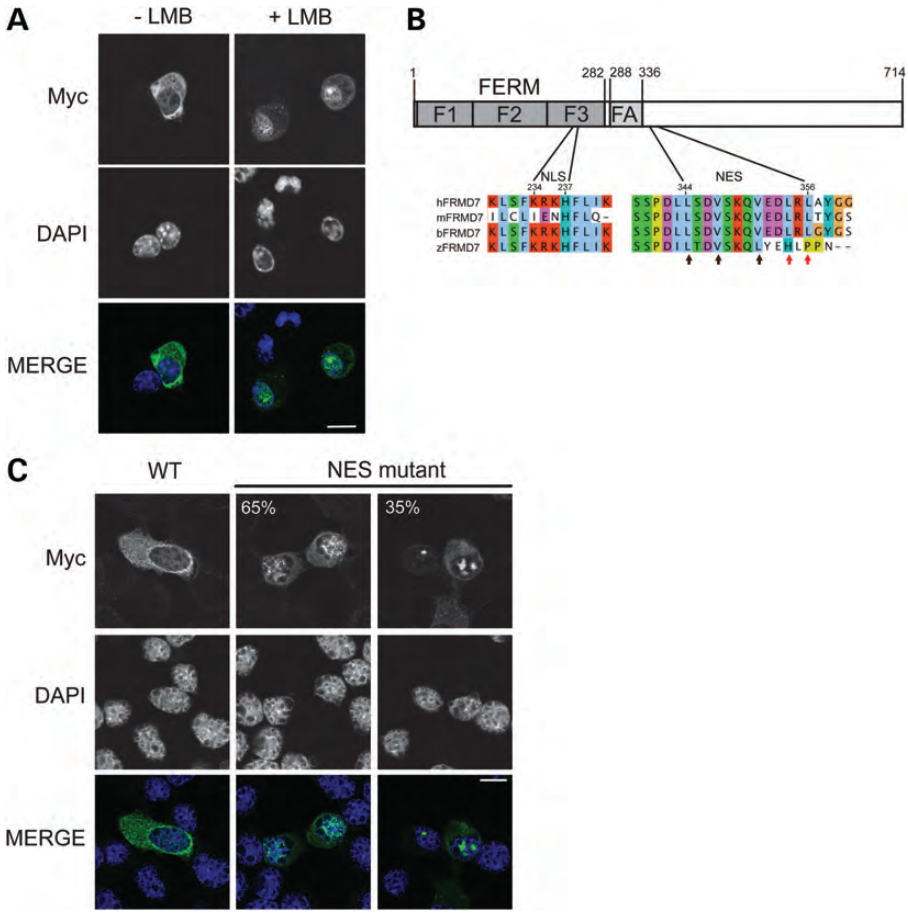

Figure 3. FRMD7 contains a functional NES and can translocate between the nucleus and cytoplasm. (**A**) Neuro2A cells were seeded onto coverslips, transiently transfected with myc-tagged WT FRMD7 and then treated with 20 nM leptomycin B (+LMB) or 70% methanol (−LMB) for 4 h before fixing in methanol. Immunofluorescence microscopy was then performed using anti-myc antibodies (green in merged image) and DAPI to stain chromatin (blue in merged image). Scale bar, 10 μm. (**B**) Schematic representation of the location of the predicted nuclear import sequence (NLS) and nuclear export sequence (NES) within FRMD7. Multiple species sequence alignments show the high degree of conservation of the motifs. Arrows indicate conserved hydrophobic residues forming the predicted NES. Red arrows indicate residues mutated in the NES mutant. (**C**) Neuro2A cells were seeded onto coverslips, transiently transfected with myc-tagged WT FRMD7 or the NES mutant (p.L354S/p.L356S) and processed for immunofluorescence microscopy as in (A). Sixty-five percent of the cells transfected with the NES mutant showed diffuse nuclear staining while 35% of the cells showed aggregation of the protein within the nucleus.

We also analyzed the effects of the FRMD7 deletion mutants on neurite outgrowth and found that overexpression of FRMD7-CTD had a minor effect on neurite formation and length, analogous to the S340L mutant (Fig. 4). In contrast, the FERM and FERM+FA mutants behaved in a similar manner to the C271Y mutant, having a dramatic dominant-negative effect on the number of neurites formed.

FRMD7 interacts with the multi-domain scaffolding protein CASK and is recruited to CASK-induced neurite outgrowths at the plasma membrane

To gain insight into the cellular pathways upon which FRMD7 acts in neuronal cells, we used a mass spectrometry approach to identify interacting partners following purification of GFP-FRMD7 from transiently transfected Neuro2A cells. One of the proteins reproducibly co-precipitated by GFP-FRMD7, but not by GFP alone, was calcium/calmodulin-dependent serine kinase (CASK). CASK is a member of the membrane-associated guanylate kinase (MAGUK) family that generally act as scaffolding proteins in synapse formation and function (23). Of relevance here, studies have shown that CASK links the neuronal plasma membrane to the actin cytoskeleton via the FERM domain protein 4.1 (24) and that it contributes to regulation of neurite outgrowth and formation of dendritic spines (25,26).

We first confirmed the interaction between GFP-FRMD7 and endogenous CASK by GFP-Trap co-precipitation and western blotting and further demonstrated that the interaction was maintained in both undifferentiated and differentiated cells (Fig. 5A). To determine which domain of FRMD7 interacts with CASK, we again detected CASK following GFP-Trap precipitation of GFP-tagged FRMD7 and deletion mutants from Neuro2A cells and, strikingly, found that CASK interacts with the FERM + FA region, but not the FERM domain alone, or the CTD (Fig. 5B). These results suggest that CASK binds to the FA domain of FRMD7.

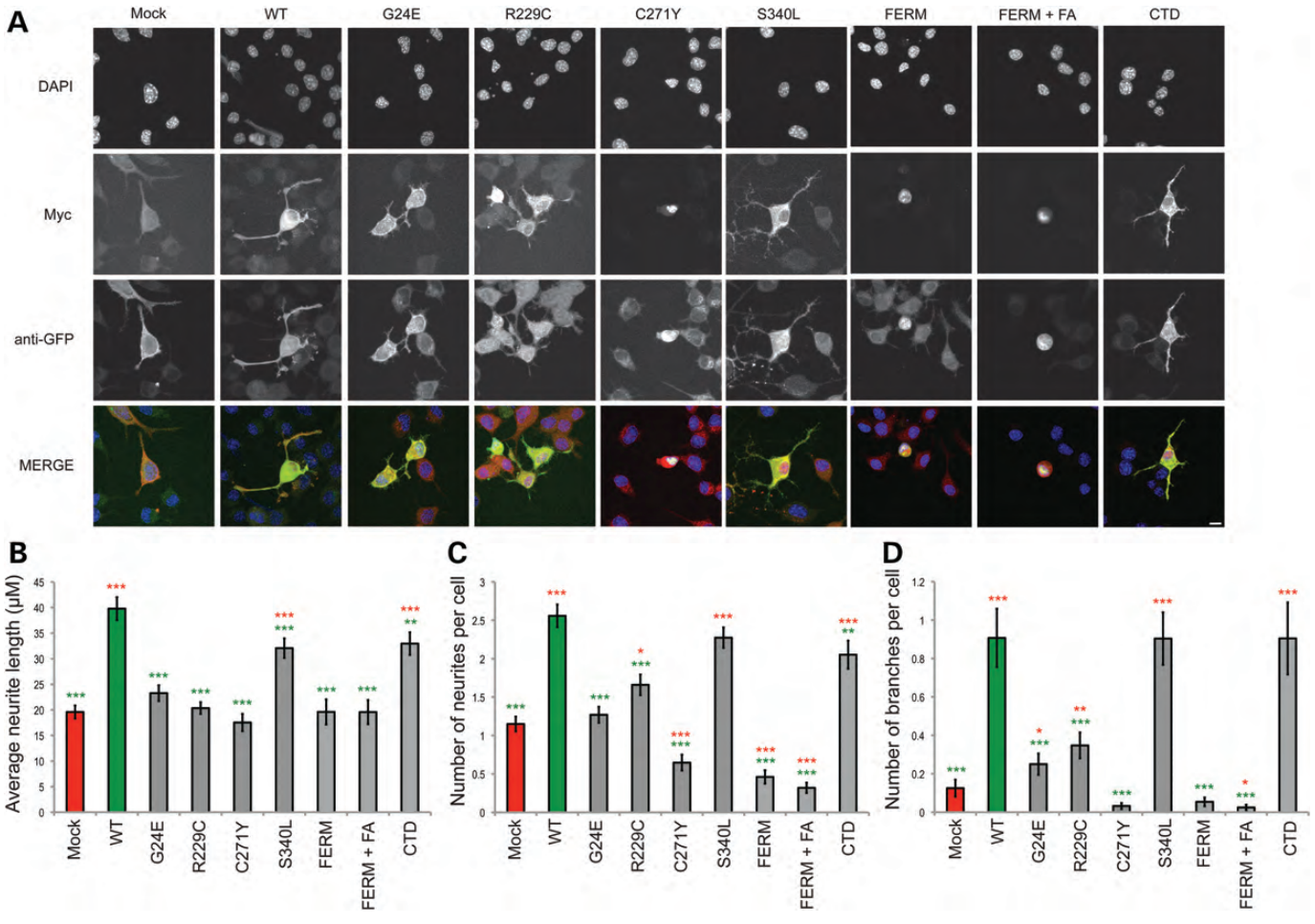

Figure 4. FRMD7 mutants inhibit the formation and extension of neurites. (**A**) Neuro2A cells were transiently co-transfected with myc-tagged WT or mutant FRMD7 together with GFP to allow visualization of neurites. The cells were replated onto coverslips 24 h after transfection and differentiated with 10 μM retinoic acid in cell-culture medium containing 2% FBS. Cells were fixed in methanol 24 h post-differentiation and immunfluorescence microscopy was performed. Cells were co-stained using anti-myc (red) and anti-GFP (green) antibodies and chromatin visualized with DAPI (blue). Representative images for each condition were captured by taking a Z-series and then flattened in Fiji so that the entire neuron could be visualized in one image. Scale bar 10 μm. (**B**–**D**) Coverslips prepared in (A) were re-analyzed using a TE300 Nikon semi-automatic microscope. Neurite lengths (B), number of neurites per cell (C) and the number of neurite branches per cell (D) were calculated from a minimum of 116 cells. The average of three experiments is shown ± S.E. $^{***}P < 0.001$, $^{**}P < 0.005$, $^{*}P < 0.05$. Red asterisks indicate significance compared with mock-transfected cells, green asterisks indicated significance compared with WT FRMD7.

We then used immunofluorescence microscopy to determine whether the two proteins co-localize in cells following exogenous expression of GFP-CASK and myc-FRMD7. In addition to general cytoplasmic localization, discrete co-localization of the proteins was observed at the plasma membrane, particularly in cells with lower expression levels of the two proteins (Fig. 5C). To confirm localization of FRMD7 to the plasma membrane, we performed biochemical fractionation of the cells and indeed observed both FRMD7 and CASK enriched in the plasma membrane fraction (Fig. 5D). Importantly, FRMD7 enrichment at the plasma membrane was observed only in the presence of overexpressed CASK. Thus, our findings indicate that CASK recruits FRMD7 to the plasma membrane.

We then examined the relative contributions of FRMD7 and CASK to neurite outgrowth in Neuro2A cells. When expressed alone in the absence of RA, GFP-CASK directly induced the extensive formation of short-membrane protrusions, as has been reported previously (25), while myc-FRMD7 overexpression had a limited effect on neurite outgrowth when expressed alone (Fig. 6). In contrast, co-expression of both proteins led to a 2-fold increase in neurite length, accompanied by a small reduction in the number of neurites compared with cells expressing CASK alone. These data suggest that FRMD7 stabilizes CASK-induced membrane protrusions and promotes their elongation.

IIN-associated mutations disrupt FRMD7 interaction with CASK, plasma membrane localization and neurite formation

To determine whether the interaction between CASK and FRMD7 is relevant to IIN disease pathophysiology, we investigated whether disease-associated mutations in FRMD7 affect binding to and co-localization with CASK. We found that all four of the FRMD7 point mutants analyzed had a significant reduction in their level of interaction with CASK (Fig. 7A and B). Interestingly, the degree of loss of interaction appeared to correlate directly with the ability of the mutants to promote

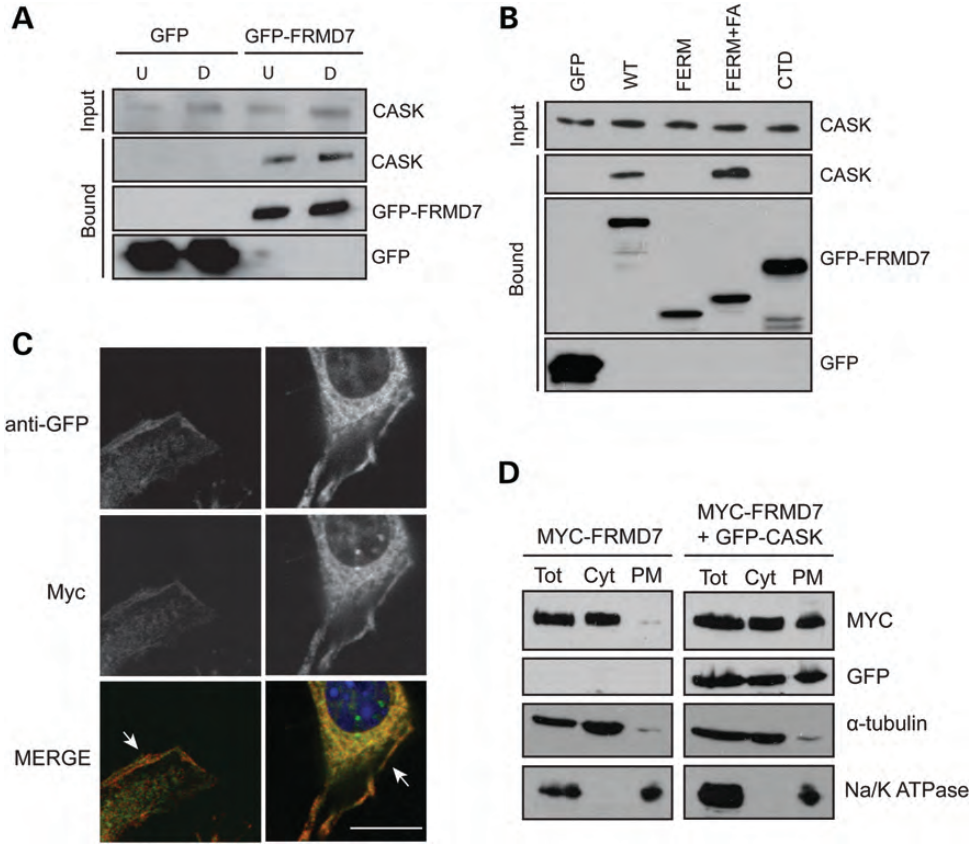

Figure 5. FRMD7 interacts and co-localizes with CASK at the plasma membrane in Neuro2A cells. (**A**) Neuro2A cells were transiently transfected with GFP or GFP-tagged FRMD7 and either treated with 10 μM retinoic acid in culture medium containing 2% FBS for 43 h to differentiate the cells (D) or they were left undifferentiated by maintaining them in culture medium containing 10% FBS (U). The GFP-tagged proteins were precipitated from cell lysates using GFP-Trap A beads and immunoblotted with anti-CASK antibodies. Precipitates were also immunoblotted with anti-GFP antibodies to confirm that the pull-downs were successful. (**B**) Neuro2A cells were transiently transfected with GFP or GFP-tagged WT FRMD7 or deletion constructs, as indicated. The GFP-tagged proteins were precipitated from cell lysates and bound CASK was detected as in (A). (**C**) Neuro2A cells were seeded onto coverslips, transiently co-transfected with myc-tagged WT FRMD7 and GFP-tagged WT CASK and then fixed in methanol 24 h later. Immunofluorescence microscopy was performed using anti-myc (green) and anti-GFP (red) antibodies and chromatin was stained with DAPI (blue). Arrows indicate areas of FRMD7 and CASK co-localization at the plasma membrane. Scale bar, 10 μm. (**D**) Neuro2A cells were transiently transfected with myc-FRMD7 alone (left panels), or in combination with GFP-CASK (right panels). Cells were harvested 24 h later and fractionated using a plasma membrane protein extraction kit. Total protein (Tot), cytoplasmic (Cyt) and plasma membrane (PM) fractions were analyzed by imunoblotting. Antibodies against α-tubulin and Na/K ATPase were used as markers of cytoplasm and plasma membrane, respectively.

neurite outgrowth (Fig. 4). Furthermore, the mutants had reduced ability to co-localize with CASK at the plasma membrane and in neurite outgrowths and appeared to inhibit formation of CASK-induced neurite outgrowths (Fig. 6C). Quantification of neurite length and numbers of neurites per cell confirmed that all mutants caused a reduction in the number of neurites formed. Furthermore, all mutants except S340L resulted in a significant reduction in neurite length. Together, these data indicate that FRMD7 localization to the plasma membrane and to neurite outgrowths depends upon its interaction with CASK and that IIN-associated FRMD7 mutations prevent this recruitment by disrupting the FRMD7–CASK interaction.

Mutations in CASK that are associated with nystagmus disrupt interaction with FRMD7

Mutations in CASK are associated with X-linked mental retardation (XLMR) but, interestingly, some individuals also present with congenital nystagmus and the mutations carried by these individuals map to C-terminal region of CASK (8,27). We hypothesized that this C-terminal region, which contains the hook and guanylate kinase (GUK) domains, may comprise the binding site for FRMD7 and that the CASK mutations found in this region disrupt interaction with FRMD7. To test this hypothesis, we used a CASK cDNA encoding an 897-residue isoform of the protein to generate a range of myc-tagged CASK point mutants [our nomenclature thus differs by 29 residues from the 919-residue isoform reported by Hackett *et al.* (8)]. These included mutants that were either associated (681–689del, Y699C, W890R) or not associated (Y268H) with nystagmus and also a deletion mutant (CASK 1–673) that lacked the C-terminal hook and GUK domains (Fig. 8A). We determined their ability to interact with GFP-FRMD7 by GFP-Trap and found that all of the nystagmus-associated CASK mutants had reduced interaction with FRMD7, while the Y268H mutant interaction was comparable with WT CASK (Fig. 8B and

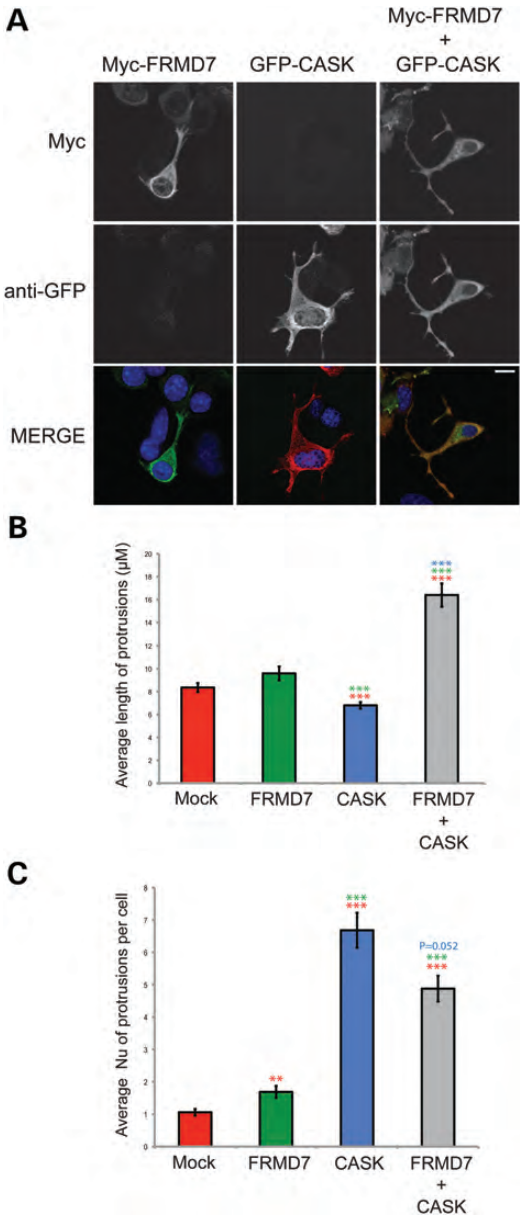

Figure 6. FRMD7 promotes elongation of CASK-induced membrane protrusions. (**A**) Neuro2A cells were seeded onto coverslips, transiently transfected with myc-tagged WT FRMD7 and GFP-tagged WT CASK, either alone or in combination, and fixed in methanol 24 h later. Immunofluorescence microscopy was performed using anti-myc (green) and anti-GFP (red) antibodies and chromatin was stained with DAPI (blue). (**B** and **C**) Coverslips prepared as in (A), except with the inclusion of empty vectors where appropriate, were analyzed using a TE300 Nikon semi-automatic microscope. Average lengths (B) and number of neurites per cell (C) were calculated from a minimum of 49 cells. The average of three experiments is shown $\pm$S.E. $^{***}P < 0.001$. Red asterisks indicate significance compared with mock-transfected cells, green asterisks indicated significance compared with cells expressing FRMD7 alone and blue asterisks indicate significance compared with CASK alone.

C). Most notably, the 681–689del and 1–673 deletion mutants both completely abolished interaction with FRMD7, confirming our hypothesis that FRMD7 binds within the C-terminal region of CASK. The relative loss of binding of the three nystagmus-associated CASK mutants further suggests that the binding site for FRMD7 lies close to the hook domain.

Together, our results demonstrate that disruption of the FRMD7–CASK interaction is a crucial step in the development of nystagmus and that this interaction is necessary for recruitment of FRMD7 to the plasma membrane and promotion of neurite outgrowth in Neuro2A cells.

DISCUSSION

In this study, we have shown that IIN-associated missense mutations in FRMD7 variably affect protein expression and localization and that they also impair neurite outgrowth. Moreover, we have identified CASK as a FRMD7 interacting partner in Neuro2A cells and demonstrated that the IIN-associated mutations lead to loss of this interaction and failure to recruit FRMD7 to the plasma membrane. These findings highlight loss of the FRMD7–CASK interaction as a major factor in the development of nystagmus.

IIN-associated mutations impair FRMD7 expression and ability to stimulate neurite outgrowth

Around 42% of FRMD7 mutations are predicted to result in loss of protein expression due to aberrant splicing and/or premature termination of protein synthesis (21) and there is evidence for this in some instances (9). For this reason, it has been hypothesized that IIN results from a null FRMD7 phenotype due to either mRNA or protein instability (9). However, our data indicate that expression of missense mutants is variable. Protein instability is likely to contribute to the disease mechanism for three of the four mutants examined, yet S340L had no apparent effect on FRMD7 protein expression. Thus, at least in some cases, it is likely that the disease arises due to loss of protein function rather than loss of expression.

We found that overexpression of FRMD7 leads to a 2-fold enhancement of RA-induced neurite outgrowth, as reported recently (28,29). This is also consistent with a previous study that demonstrated reduced neurite length after down-regulation of FRMD7 (20). Loss of FRMD7 function in some cases of IIN is supported by our finding that, although apparently localized normally within the cytoplasm, the G24E, R229C and, to a lesser extent, S340L mutants failed to enhance neurite outgrowth to the same extent as WT FRMD7. While this could be ascribed to the lower level of mutant protein expression, it should be noted that only cells with clearly detectable FRMD7 expression were included for neurite length analysis (Fig. 4).

In contrast to the other mutations examined, C271Y caused FRMD7 accumulation in the nucleus and further analysis revealed that FRMD7 contains an NES located immediately downstream of the FA domain. It is therefore possible that C271Y exposes a cryptic NLS. Alternatively, the mutation may disrupt the conformation of the NES, which has been shown to adopt an α-helical structure in other proteins (30,31), thus preventing binding to CRM1. The importance of the NES is highlighted by the fact that C-terminal deletion mutants that lack the NES are generally localized in the nucleus, as has also been observed by Pu *et al*. (32). Since

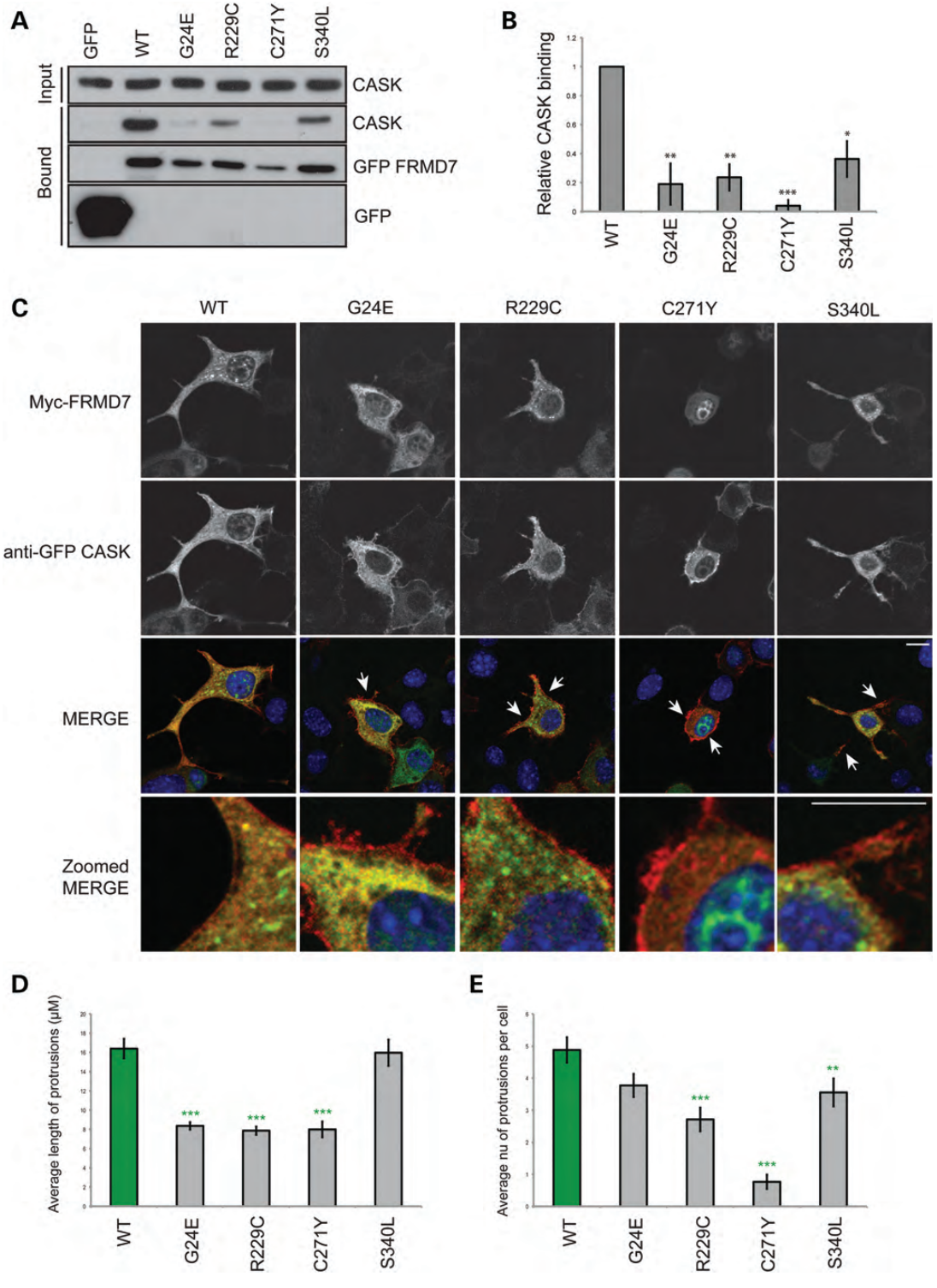

Figure 7. IIN associated mutations disrupt the interaction between FRMD7 and CASK. (**A**) Neuro2A cells were transiently transfected with GFP-tagged WT FRMD7 or IIN-associated mutants (G24E, R229C, C271Y and S340L). Twenty-four hours post-transfection, GFP-Trap A beads were used to precipitate the GFP-tagged proteins and co-precipitating CASK was detected by immunoblotting, (**B**) Binding of CASK to each mutant was quantified by densitometry with respect to the amount of each FRMD7 mutant precipitated and is expressed relative to the value obtained for WT FRMD7. The average of three experiments is shown $\pm$S.E. $^{*}P < 0.05$; $^{**}P < 0.01$; $^{***}P < 0.001$. (**C**) Neuro2A cells were seeded onto coverslips and transiently co-transfected with GFP-CASK and either WT myc-FRMD7 or IIN mutants and then fixed in methanol. Immunofluorescence microscopy was performed and transfected proteins detected using anti-myc (green) and anti-GFP (red) antibodies. Chromatin was visualized with DAPI (blue). Arrows highlight areas in the membrane in which CASK and FRMD7 fail to co-localize. Representative images from three experiments are shown. Scale bar, 10 μm. (**D** and **E**) Coverslips from (C) were analyzed using a TE300 Nikon semi-automatic microscope. Average lengths (D) and number of protrusions per cell (E) were calculated from a minimum of 43 cells. The average of three experiments is shown $\pm$S.E. $^{***}P < 0.001$; $^{**}P < 0.001$. Green asterisks indicate significance compared with wild-type (WT) FRMD7.

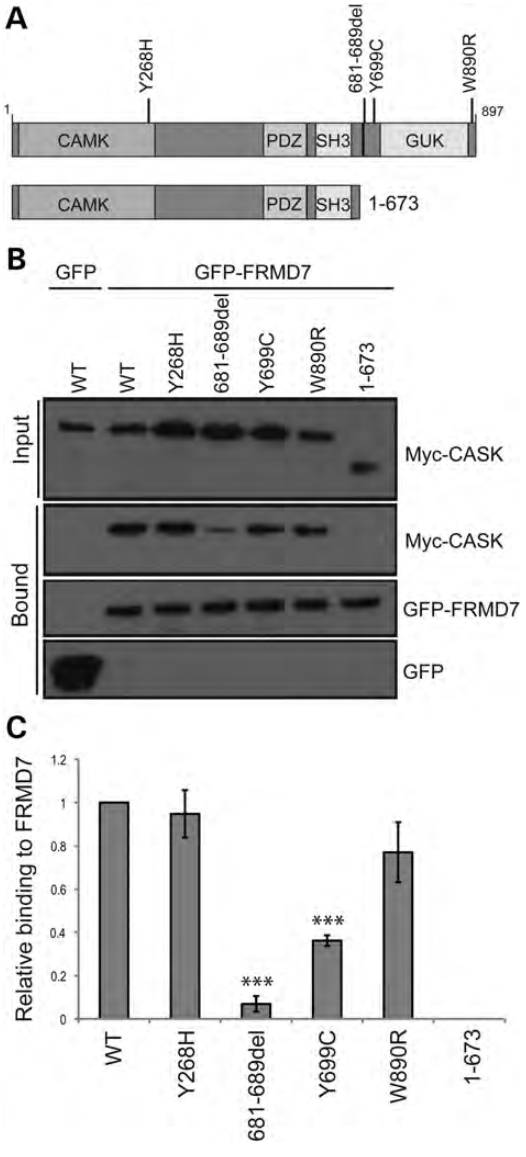

Figure 8. CASK mutants associated with XLMR and nystagmus disrupt the interaction between FRMD7 and CASK. (**A**) Schematic representation of the domain organization of CASK and deletion mutant 1-673. CAMK, calmodulin kinase-like domain; GUK, guanylate kinase domain. Black bar indicates the hook domain. The mutants used in the study are indicated. Sequences are based on the CASK isoform that encodes 897 residues (ENST00000421587) and lacks residues 340–345 and 580–602 compared with the 926-residue isoform reported by Hackett *et al*. (8). (**B**) Neuro2A cells were transiently co-transfected with GFP-tagged WT FRMD7 and myc-tagged WT or mutant CASK. Twenty-four hours post-transfection, GFP-Trap A beads were used to precipitate the GFP-FRMD7 and co-precipitating CASK was detected by immunoblotting. (**C**) Binding of WT and mutant CASK to FRMD7 was quantified by densitometry with respect to CASK input and bound FRMD7 and is expressed relative to the value obtained for wild-type CASK. The average of three experiments is shown $\pm$S.E. $^{***}P < 0.001$.

many IIN mutations in FRMD7 result in premature protein termination, this could be a common feature of the disease.

As FRMD7 is predominantly localized and thought to function within the cytoplasm, it would be expected that sequestration of the C271Y mutant within the nucleus would result in a loss-of-function phenotype. However, this mutant had a strong dominant-negative effect on neurite outgrowth. Together with the even more dramatic effects of the FERM domain truncation mutant, this suggests that nuclear localization of FRMD7 is highly deleterious to the cell and to neurite outgrowth. The reason for this effect is currently unclear, but could be due to alternative functions of FRMD7 within the nucleus at particular developmental stages (see in what follows).

FRMD7 interaction with CASK in neuronal function

CASK is a widely expressed but brain-enriched member of the MAGUK family that act as scaffolds for protein-complex formation at cell junctions, including neuronal synapses (23). CASK comprises at least six protein–protein interaction domains allowing assembly of large multi-protein complexes at the plasma membrane and it has been implicated in both neuronal development and synaptic function (33). The PDZ domain interacts with the C-termini of plasma membrane adhesion proteins, including neurexins and syndecans (24,34). Of particular relevance to FRMD7 function, CASK has been shown to interact with the founding member of the FERM domain family, protein 4.1, via the short hook motif located close to its C-terminus (24,34). Thus, one of the functions of CASK in neurons is to link the plasma membrane to the actin cytoskeleton. Furthermore, CASK has been shown to stabilize dendritic spines, a function that requires both its syndecan-2 and protein 4.1 binding sites, suggesting that these interactions play a major role in synapse formation (25).

We demonstrated that CASK recruits FRMD7 to the plasma membrane. Furthermore, over-expression of FRMD7 reduced the number of CASK-induced neurites, but these neurites were longer, suggesting a role for the FRMD7–CASK interaction in the stabilization and elongation of neurites, analogous to protein 4.1 (25). This is also supported by the report that RNAi-mediated down-regulation of FRMD7 leads to increased neurite number, but decreased neurite length (20).

We mapped the binding site for CASK to the FA domain of FRMD7, although we cannot rule out the possibility that sequences within the FERM domain also contribute to the interaction. The FA domain is found in a subset of FERM domain proteins and has been postulated to be a regulatory domain. Two serines located in the FA domain of protein 4.1R have been shown to be targets for phosphorylation by PKA and PKC and are conserved in around half of the known FERM-domain proteins (13). Although these sites are not found in FRMD7, multiple conserved serine and threonine residues are present within the FA domain and phosphorylation of one of these residues could represent a means of regulation of the CASK–FRMD7 interaction.

Interestingly, post-translational modification of CASK has been shown to regulate its activities. SUMOylation of the SH3 domain of CASK, close to the hook domain (Fig. 8), regulates its interaction with protein 4.1 (25), while phosphorylation by CDK5 promotes recruitment of CASK to the synaptic membrane. CASK also has roles in regulating neuronal gene expression within the nucleus and phosphorylation of the C-terminal GUK domain by PKA regulates an interaction with transcription factor Tbr-1 (35). In embryonic neurons, around 20% of CASK is found in the nucleus but this localization is lost in adult neurons (36). It is tempting to speculate that modulation of

the activity of the FRMD7 NES, potentially through phosphorylation, could influence its nuclear localization during brain development. In this regard, it is interesting to note that protein 4.1 has been detected in the nucleus as part of a filamentous network (37). An alternative possibility is that the NES constitutively prevents accumulation of FRMD7 in the nucleus, where it could interfere with the alternative functions of CASK during brain development.

Unexpectedly, we found that the isolated FRMD7 CTD was able to stimulate neurite outgrowth to the same extent as full-length FRMD7. One explanation for this is that the FERM domain may hold the CTD in an inactive conformation until it has bound the appropriate factors, including CASK, at the plasma membrane. The isolated CTD may be relieved of this inhibition and thus become free to stimulate the necessary rearrangement of the actin cytoskeleton to promote membrane extension. The function of the CTD is currently unknown, but is likely to involve regulation of actin remodeling (20).

Role of the FRMD7-CASK interaction in IIN

Our data indicate that the interaction between FRMD7 and CASK is crucial for correct development of oculomotor control since mutations in either protein that disrupt their interaction result in nystagmus. Mutations in CASK result in XLMR but, importantly, only those found within the C-terminal region of CASK additionally cause nystagmus (8). These findings allow us to locate the binding site for FRMD7 to the C-terminus of CASK. Moreover, the two closely apposed mutations, 681–689del and Y699C, which are located immediately adjacent to the hook motif, caused a more severe reduction in interaction with FRMD7 than W890R. This suggests that, like protein 4.1, FRMD7 binds to the hook motif of CASK (34).

IIN-associated mutations prevented FRMD7 recruitment to the plasma membrane of CASK-induced neurites and spines, indicating that FRMD7 is dependent on interaction with CASK for its localization at the plasma membrane. Thus we can propose a model whereby, during development of the neural network that controls eye movement, FRMD7 is recruited to the plasma membrane by interaction with CASK, potentially aided by membrane receptors such as syndecans or neurexins. FRMD7 then promotes localized remodeling of the actin cytoskeleton to allow stabilization and extension of membrane protrusions that lead to axonogenesis and dendritogenesis. A role for FRMD7 in cytoskeletal remodeling is supported by recent demonstrations that over-expression of FRMD7 leads to up-regulation of genes encoding cytoskeletal proteins (29) while RNAi-mediated knock-down results in altered actin dynamics (20).

FRMD7 expression is not restricted to the oculomotor control center of the brain and so it is perhaps surprising that defects in FRMD7 function do not result in more widespread defects in brain development. One possible explanation for this is that there is functional redundancy in other parts of the brain, with additional FERM domain proteins fulfilling the same role of binding to CASK. FARP1 and FARP2 are potential binding partners in other neuronal cells since they also participate in regulating the growth of axons and dendrites (17,18).

Clinical versus biochemical phenotype correlations

We observed a clear distinction between the four disease-associated FRMD7 point mutants in terms of the severity of biochemical and cellular defects. C271Y had the most dramatic effects, resulting in poor protein expression, aberrant localization to the nucleus and dominant-negative inhibition of neurite outgrowth. Furthermore, interaction with CASK was completely abolished. In all these aspects, the G24E and R229C mutants had an intermediate effect. At the opposite extreme, S340L caused only mild defects in FRMD7 expression and ability to promote neurite outgrowth, and interaction with CASK was less severely perturbed. Importantly, these biochemical defects appear to correlate with the severity of vision impairment of IIN patients carrying these mutations. Previous studies have shown that the median visual acuity among patients with *FRMD7* mutations was 0.2 LogMAR (range 0.0–0.54 LogMAR) (3,10). Interestingly, a patient carrying the S340L mutation had better visual acuity (0.1 LogMAR) than the median visual acuity of the cohort, while affected members of a family carrying the C271Y mutation had poorer median visual acuity (0.38 LogMAR) (10). Since *FRMD7* mutations are rare and each mutation only found in a single family, further statistical analysis is so far not possible.

Previous studies have identified a range of phenotypical characteristics associated with CASK mutations (8,27). The ocular phenotypical characteristics include nystagmus, reduced visual acuity and strabismus. Interestingly, the W890R CASK variant [referred to as W919R by Hackett *et al*. (8)] was associated with milder visual impairment (none of the affected patients had a reduced visual acuity) in comparison with the other nystagmus-associated CASK mutations (8). This again could be explained by the fact that the W890R variant caused a weaker reduction of the FRMD7–CASK interaction compared with the other nystagmus-associated CASK mutants tested (Fig. 8).

These correlations suggest that the biochemical defects that we have observed are directly related to the clinical phenotype. However, large-scale genotype–phenotype correlation studies are needed to confirm these findings. Our data suggest that nuclear localizing FRMD7 mutants are likely to result in a more severe clinical phenotype. Since over 40% of FRMD7 mutations lead to premature protein truncation, these mutants would also be expected to localize to the nucleus, as recently demonstrated for the R335X mutant (32).

Further studies are required to understand how the CASK–FRMD7 interaction is controlled during neuronal development and to identify downstream cytoskeletal targets of FRMD7. Importantly, the gene encoding CASK lies within one of the mapped loci for nystagmus, at Xp11.3–11.4, and should therefore be considered as a strong candidate gene in families whose disease maps to this chromosomal location, particularly if associated with mental retardation.

MATERIALS AND METHODS

Plasmids

The human FRMD7 cDNA, encoding the 714-residue full-length protein, was obtained by PCR amplification from

IMAGE clone 40 079 764 and inserted into pLEICS-20 (N-terminal myc tag) and pLEICS-21 (N-terminal GFP tag) mammalian expression vectors by recombination-based cloning, using the University of Leicester Protex cloning service. The human CASK cDNA, encoding the 897-residue protein, was similarly amplified by PCR from IMAGE clone 9051964 and inserted into pLEICS-20 and pLEICS-21 mammalian expression vectors. Disease-associated point mutations were introduced by site-directed mutagenesis using the Quickchange site-directed mutagenesis kit (Invitrogen) as per manufacturer's instructions. Deletion mutants were created by PCR amplification of regions from the appropriate IMAGE clone encoding the required residues and recombination into pLEICS-20 and pLEICS-21.

Cell culture, transfection and drug treatments

Neuro2A cells (CCL-131, ATCC) were routinely grown in Dulbecco's modified Eagle medium (DMEM) supplemented with 10% FBS and antibiotics at 37°C and 5% CO_2. Cells were transiently transfected using Lipofectamine 2000 (Invitrogen), according to the manufacturer's instructions. To induce differentiation, cells were cultured in DMEM supplemented with 2% FBS, antibiotics and 10 μM RA (Sigma) for 24 or 48 h. For studies investigating the nuclear localization of FRMD7, cells were treated with 20 nM leptomycin B (Sigma) for 4 h prior to harvesting.

Antibodies

Rabbit FRMD7 (HPA000886) and mouse α-tubulin antibodies were obtained from Sigma. Mouse CASK (C-6) and myc-tag (9E10) antibodies were purchased from Santa Cruz and Invitrogen, respectively. Rabbit GFP-tag (ab6556) and mouse Na/K ATPase (ab7671) antibodies were obtained from Abcam. Mouse GAPDH (6C5) antibodies were purchased from Millipore.

Cell extracts, GFP-Trap and immunoblotting

Neuro2A cells were grown to 90% confluence on 10 cm dishes, transfected with the appropriate FRMD7 and/or CASK constructs and harvested 24–48 h later. For GFP-Trap, cell extracts were harvested by incubating the cells in lysis buffer [50 mM HEPES (pH7.4), 1 mM phenylmethylsulfonyl fluoride (PMSF), 1% NP40, 150 mM NaCl, 5 mM NaF, 50 mM β-glycerophosphate containing complete protease inhibitor cocktail (Roche)] for 30 min at 4°C. Cells were removed from the plates by scraping, briefly sonicated and centrifuged at 20 000 *g* for 10 min at 4°C. GFP-tagged proteins were precipitated by incubating the soluble lysates with GFP-Trap A beads (Chromotek) for 2 h at 4°C. The beads were pelleted at 2000 *g* and then washed in dilution buffer [10 mM Tris–HCl (pH 7.4), 150 mM NaCl, 0.5 mM EDTA, 1 mM PMSF, 5 mM NaF, 50 mM β-glycerophosphate containing complete protease inhibitor cocktail (Roche)].

For plasma membrane fractionation, cells were harvested and processed 24 h post-transfection using a plasma membrane protein extraction kit (Abcam), according to the manufacturer's instructions.

For immunoblotting, samples were boiled in an equal volume of 2 × Laemmli buffer, resolved on 7.5 or 10% SDS–polyacrylamide gels and transferred to nitrocellulose membrane. Membranes were probed using the appropriate primary antibodies and dilutions: FRMD7 (1:700), CASK (1:500), GFP (1:8000), Myc (1:500), Na/K ATPase (1:2000), GAPDH (1:10 000) or α-tubulin (1:10 000). Primary antibodies were detected with horseradish peroxidase-conjugated anti-rabbit or anti-mouse secondary antibodies (Sigma) and visualization was performed using ECL reagents (Geneflow).

Mass spectrometry

Proteomics was carried out by the University of Leicester Proteomics Facility (PNACL, University of Leicester). Following GFP-Trap, samples were resolved on 10% polyacrylamide gels and stained with Brilliant Blue G-Colloidal concentrate electrophoresis reagent (Sigma). In-gel trypsin digestion was carried out upon excised bands of interest. The identity of the band corresponding to the molecular weight of GFP-FRMD7 was confirmed by MALDI-ToF mass spectrometry using a Voyager DE-STR mass spectrometer (Applied Biosystems). Interacting proteins were determined by LC–MS/MS using an RSLCnano HPLC system (Dionex, UK) and an LTQ-Orbitrap-Velos mass spectrometer (Thermo Scientific). Samples were loaded at high flow-rate onto a reverse-phase trap column (0.3 mm i.d. × 1 mm), containing 5 μm C18 300 Å Acclaim PepMap media (Dionex) maintained at a temperature of 37°C. The loading buffer was 0.1% formic acid/0.05% trifluoroacetic acid/2% acetonitrile.

The raw data file obtained from each LC–MS/MS acquisition was processed using Proteome Discoverer (version 1.3, Thermo Scientific), searching each file in turn using Mascot (version 2.2.04, Matrix Science Ltd) against a database containing the UniProtKB/Swissprot accessions for *Homo sapiens*. The peptide tolerance was set to 5 ppm and the MS/MS tolerance was set to 0.02 Da. The output from Proteome Discoverer was further processed using Scaffold Q + S (version 3.6.1, Proteome Software). Upon import, the data were searched using X!Tandem (The Global Proteome Machine Organization). PeptideProphet and ProteinProphet (Institute for Systems Biology) probability thresholds of 95% were calculated from the decoy searches and Scaffold was used to calculate an improved 95% peptide and protein probability threshold based on the data from the two different search algorithms.

Immunofluorescence microscopy

Neuro2A cells were grown on acid-treated coverslips and fixed with methanol at −20°C for 20 min. Following fixation, coverslips were washed three times with PBS, blocked with 1% bovine serum albumin (BSA) in PBS for 10 min and washed again three times in PBS. All subsequent antibody incubations were carried out for 1 h in PBS containing 3% BSA. Primary antibodies were Myc (1:500) and GFP (1:500). Primary antibody incubations were followed by three washes with PBS. Detection of primary antibodies was carried out using the following secondary antibodies: donkey anti-mouse AlexaFluor 488 and donkey anti-rabbit AlexaFluor

594 (Invitrogen). All secondary antibodies had been tested and found to be negative for cross-reactivity. DNA was stained with 50 ng/μl 4,6 diamidino-2-phenylindol (DAPI; Invitrogen). Following three final washes in PBS, coverslips were mounted in 80% glycerol-3% *n*-propyl gallate (in PBS) or Prolong Gold antifade reagent (Invitrogen). Fluorescence microscopy was performed with a Leica TCS SP5 laser scanning confocal microscope and a 63 × objective, using LAS-AF software. Alexa 488 was excited using the 488 nm laser line and emissions collected between 500 and 590 nm. DAPI and Alexa 594 were similarly excited using the 405 or 594 nm laser lines and emissions collected between 415 and 480 nm, or 605 and 700 nm, respectively. Images (8-bit) were processed with Adobe Photoshop (Adobe Systems) and Fiji (38).

Quantification of neurite outgrowth

Neurite outgrowth was observed 24 h post-RA-induced differentiation of transiently transfected Neuro2A cells. Fluorescence images of transfected cells were captured with a TE300 Nikon semi-automatic microscope using a 40 × objective with an ORCA-R^2 charge-couple device camera (Hamamatsu) and Volocity software (PerkinElmer). Neurites were traced manually in Fiji using the Simple Neurite Tracer plug-in (39). Statistics were gathered on the average neurite length per cell (sum of primary neurite and branch length), the number of neurites per cell and the number of neurite branches per cell. A neurite is defined as an outgrowth with a length more than half the diameter of the cell body and a neurite branch is defined as a neurite with secondary neurites arising from the primary neurite. At least 116 cells per transfection were scored for neurite outgrowth. Statistical significance was determined using a Mann–Whitney test.

Protein structure modeling

Structural homology models were generated using PHYRE (22) and the FRMD7 sequence 1–280. The best model was obtained using the structure of the FERM domain of protein 4.1R (PDB ID: 1GG3). Sequence alignment of the amino-acid sequence of human FRMD7 (Q6ZUT3) with the FERM domain of protein 4.1R (residues 210–488) was carried out using T-coffee (40). T-coffee alignment suggests a good match throughout the aligned region with a score of 98 and comparison of the model with the protein 4.1R structure confirmed its reliability.

ACKNOWLEDGEMENTS

We thank the University of Leicester Protex cloning facility for generation of plasmid constructs and A. Bottrill (PNACL proteomics service, University of Leicester) for help and advice with MS data analysis. We are grateful to K. Straatman (Advanced Imaging Facility, University of Leicester) for help with imaging and to C. Talbot for assistance with statistical analysis. We also thank S. Macip for generously providing reagents for the plasma membrane purification studies and J. Schwabe for helpful discussions and critical reading of the manuscript

Conflict of Interest statement. None declared.

FUNDING

This work was supported by funding from the Ulverscroft Foundation (awarded to I.G.) and from the Wellcome Trust (awarded to S.S.). Funding to pay the Open Access publication charges for this article was provided by the Leverhulme Trust and Wellcome Trust.

REFERENCES

1. Ehrt, O. (2012) Infantile and acquired nystagmus in childhood. *Eur. J. Paed. Neurol.*, **16**, 567–572.
2. Sarvananthan, N., Surendran, M., Roberts, E.O., Jain, S., Thomas, S., Shah, N., Proudlock, F.A., Thompson, J.R., McLean, R.J., Degg, C. *et al.* (2009) The prevalence of nystagmus: the Leicestershire nystagmus survey. *Invest. Ophthalmol. Vis. Sci.*, **50**, 5201–5206.
3. Thomas, S., Proudlock, F.A., Sarvananthan, N., Roberts, E.O., Awan, M., McLean, R., Surendran, M., Kumar, A.S., Farooq, S.J., Degg, C. *et al.* (2008) Phenotypical characteristics of idiopathic infantile nystagmus with and without mutations in FRMD7. *Brain*, **131**, 1259–1267.
4. Harris, C. and Berry, D. (2006) A developmental model of infantile nystagmus. *Semin. Ophthalmol.*, **21**, 63–69.
5. Cabot, A., Rozet, J.M., Gerber, S., Perrault, I., Ducroq, D., Smahi, A., Souied, E., Munnich, A. and Kaplan, J. (1999) A gene for X-linked idiopathic congenital nystagmus (NYS1) maps to chromosome Xp11.4-p11.3. *Am. J. Hum. Genet.*, **64**, 1141–1146.
6. Kerrison, J.B., Vagefi, M.R., Barmada, M.M. and Maumenee, I.H. (1999) Congenital motor nystagmus linked to Xq26-q27. *Am. J. Hum. Genet.*, **64**, 600–607.
7. Bassi, M.T., Schiaffino, M.V., Renieri, A., De Nigris, F., Galli, L., Bruttini, M., Gebbia, M., Bergen, A.A., Lewis, R.A. and Ballabio, A. (1995) Cloning of the gene for ocular albinism type 1 from the distal short arm of the X chromosome. *Nat. Genet.*, **10**, 13–19.
8. Hackett, A., Tarpey, P.S., Licata, A., Cox, J., Whibley, A., Boyle, J., Rogers, C., Grigg, J., Partington, M., Stevenson, R.E. *et al.* (2010) CASK mutations are frequent in males and cause X-linked nystagmus and variable XLMR phenotypes. *Eur. J. Hum. Genet.*, **18**, 544–552.
9. Tarpey, P., Thomas, S., Sarvananthan, N., Mallya, U., Lisgo, S., Talbot, C.J., Roberts, E.O., Awan, M., Surendran, M., McLean, R.J. *et al.* (2006) Mutations in FRMD7, a newly identified member of the FERM family, cause X-linked idiopathic congenital nystagmus. *Nat. Genet.*, **38**, 1242–1244.
10. Thomas, M.G., Crosier, M., Lindsay, S., Kumar, A., Thomas, S., Araki, M., Talbot, C.J., McLean, R.J., Surendran, M., Taylor, K. *et al.* (2011) The clinical and molecular genetic features of idiopathic infantile periodic alternating nystagmus. *Brain*, **134**, 892–902.
11. Self, J.E., Shawkat, F., Malpas, C.T., Thomas, N.S., Harris, C.M., Hodgkins, P.R., Chen, X., Trump, D. and Lotery, A.J. (2007) Allelic variation of the FRMD7 gene in congenital idiopathic nystagmus. *Arch. Ophthalmol.*, **125**, 1255–1263.
12. Chishti, A.H., Kim, A.C., Marfatia, S.M., Lutchman, M., Hanspal, M., Jindal, H., Liu, S.C., Low, P.S., Rouleau, G.A., Mohandas, N. *et al.* (1998) The FERM domain: a unique module involved in the linkage of cytoplasmic proteins to the membrane. *Trends Biochem. Sci.*, **23**, 281–282.
13. Baines, A.J. (2006) A FERM-adjacent (FA) region defines a subset of the 4.1 superfamily and is a potential regulator of FERM domain function. *BMC Genomics*, **7**, 85.
14. Diakowski, W., Grzybek, M. and Sikorski, A.F. (2006) Protein 4.1, a component of the erythrocyte membrane skeleton and its related homologue proteins forming the protein 4.1/FERM superfamily. *Folia Histochem. Cytobiol.*, **44**, 231–248.
15. Kubo, T., Yamashita, T., Yamaguchi, A., Sumimoto, H., Hosokawa, K. and Tohyama, M. (2002) A novel FERM domain including guanine nucleotide exchange factor is involved in Rac signaling and regulates neurite remodeling. *J. Neurosci.*, **22**, 8504–8513.
16. Takegahara, N., Kang, S., Nojima, S., Takamatsu, H., Okuno, T., Kikutani, H., Toyofuku, T. and Kumanogoh, A. (2010) Integral roles of a

guanine nucleotide exchange factor, FARP2, in osteoclast podosome rearrangements. *FASEB J.*, **24**, 4782–4792.
17. Toyofuku, T., Yoshida, J., Sugimoto, T., Zhang, H., Kumanogoh, A., Hori, M. and Kikutani, H. (2005) FARP2 triggers signals for Sema3A-mediated axonal repulsion. *Nat. Neurosci.*, **8**, 1712–1719.
18. Zhuang, B., Su, Y.S. and Sockanathan, S. (2009) FARP1 promotes the dendritic growth of spinal motor neuron subtypes through transmembrane Semaphorin6A and PlexinA4 signaling. *Neuron*, **61**, 359–372.
19. Self, J., Haitchi, H.M., Griffiths, H., Holgate, S.T., Davies, D.E. and Lotery, A. (2010) Frmd7 expression in developing mouse brain. *Eye*, **24**, 165–169.
20. Betts-Henderson, J., Bartesaghi, S., Crosier, M., Lindsay, S., Chen, H.L., Salomoni, P., Gottlob, I. and Nicotera, P. (2010) The nystagmus-associated FRMD7 gene regulates neuronal outgrowth and development. *Hum. Mol. Genet.*, **19**, 342–351.
21. Watkins, R.J., Thomas, M.G., Talbot, C.J., Gottlob, I. and Shackleton, S. (2012) The role of FRMD7 in idiopathic infantile nystagmus. *J. Ophthalmol.*, **2012**, 460956.
22. Kelley, L.A. and Sternberg, M.J. (2009) Protein structure prediction on the Web: a case study using the Phyre server. *Nat. Protoc.*, **4**, 363–371.
23. Zheng, C.Y., Seabold, G.K., Horak, M. and Petralia, R.S. (2011) MAGUKs, synaptic development, and synaptic plasticity. *Neuroscientist*, **17**, 493–512.
24. Biederer, T. and Sudhof, T.C. (2001) CASK and protein 4.1 support F-actin nucleation on neurexins. *J. Biol. Chem.*, **276**, 47869–47876.
25. Chao, H.W., Hong, C.J., Huang, T.N., Lin, Y.L. and Hsueh, Y.P. (2008) SUMOylation of the MAGUK protein CASK regulates dendritic spinogenesis. *J. Cell Biol.*, **182**, 141–155.
26. Kuo, T.Y., Hong, C.J., Chien, H.L. and Hsueh, Y.P. (2010) X-linked mental retardation gene CASK interacts with Bcl11A/CTIP1 and regulates axon branching and outgrowth. *J. Neurosci. Res.*, **88**, 2364–2373.
27. Tarpey, P.S., Smith, R., Pleasance, E., Whibley, A., Edkins, S., Hardy, C., O'Meara, S., Latimer, C., Dicks, E., Menzies, A. *et al.* (2009) A systematic, large-scale resequencing screen of X-chromosome coding exons in mental retardation. *Nat. Genet.*, **41**, 535–543.
28. Li, Y., Pu, J., Liu, Z., Xu, S., Jin, F., Zhu, L., Tian, J., Luo, J. and Zhang, B. (2011) Identification of a novel FRMD7 splice variant and functional analysis of two FRMD7 transcripts during human NT2 cell differentiation. *Mol. Vis.*, **17**, 2986–2996.
29. Pu, J., Lu, X., Zhao, G., Yan, Y., Tian, J. and Zhang, B. (2012) FERM domain containing protein 7 (FRMD7) upregulates the expression of neuronal cytoskeletal proteins and promotes neurite outgrowth in Neuro-2a cells. *Mol. Vis.*, **18**, 1428–1435.
30. Dong, X., Biswas, A., Suel, K.E., Jackson, L.K., Martinez, R., Gu, H. and Chook, Y.M. (2009) Structural basis for leucine-rich nuclear export signal recognition by CRM1. *Nature*, **458**, 1136–1141.
31. Guttler, T., Madl, T., Neumann, P., Deichsel, D., Corsini, L., Monecke, T., Ficner, R., Sattler, M. and Gorlich, D. (2010) NES consensus redefined by structures of PKI-type and Rev-type nuclear export signals bound to CRM1. *Nat. Struct. Mol. Biol.*, **17**, 1367–1376.
32. Pu, J., Li, Y., Liu, Z., Yan, Y., Tian, J., Chen, S. and Zhang, B. (2011) Expression and localization of FRMD7 in human fetal brain, and a role for F-actin. *Mol. Vis.*, **17**, 591–597.
33. Hsueh, Y.P. (2006) The role of the MAGUK protein CASK in neural development and synaptic function. *Curr. Med. Chem.*, **13**, 1915–1927.
34. Cohen, A.R., Woods, D.F., Marfatia, S.M., Walther, Z., Chishti, A.H. and Anderson, J.M. (1998) Human CASK/LIN-2 binds syndecan-2 and protein 4.1 and localizes to the basolateral membrane of epithelial cells. *J. Cell Biol.*, **142**, 129–138.
35. Huang, T.N., Chang, H.P. and Hsueh, Y.P. (2010) CASK phosphorylation by PKA regulates the protein-protein interactions of CASK and expression of the NMDAR2b gene. *J. Neurochem.*, **112**, 1562–1573.
36. Hsueh, Y.P., Wang, T.F., Yang, F.C. and Sheng, M. (2000) Nuclear translocation and transcription regulation by the membrane-associated guanylate kinase CASK/LIN-2. *Nature*, **404**, 298–302.
37. Kiseleva, E., Drummond, S.P., Goldberg, M.W., Rutherford, S.A., Allen, T.D. and Wilson, K.L. (2004) Actin- and protein-4.1-containing filaments link nuclear pore complexes to subnuclear organelles in Xenopus oocyte nuclei. *J. Cell Sci.*, **117**, 2481–2490.
38. Schindelin, J., Arganda-Carreras, I., Frise, E., Kaynig, V., Longair, M., Pietzsch, T., Preibisch, S., Rueden, C., Saalfeld, S., Schmid, B. *et al.* (2012) Fiji: an open-source platform for biological-image analysis. *Nat. Methods*, **9**, 676–682.
39. Longair, M.H., Baker, D.A. and Armstrong, J.D. (2011) Simple Neurite Tracer: open source software for reconstruction, visualization and analysis of neuronal processes. *Bioinformatics*, **27**, 2453–2454.
40. Notredame, C., Higgins, D.G. and Heringa, J. (2000) T-Coffee: a novel method for fast and accurate multiple sequence alignment. *J. Mol. Biol.*, **302**, 205–217.